2-2010

Two-dimensional Fast Surface Imaging Using a Handheld Optical Device: In Vitro and In Vivo Fluorescence Studies

Sarah J. Erickson
Department of Biomedical Engineering, Florida International University

Jiajia Ge
Department of Biomedical Engineering, Florida International University

Andrea Sanchez
Department of Biomedical Engineering, Florida International University

Anuradha Godavarty
Department of Biomedical Engineering, Florida International University, godavart@fiu.edu

Translational Oncology
www.transonc.com

Volume 3 Number 1 February 2010 pp. 16–22 16

Two-dimensional Fast Surface Imaging Using a Handheld Optical Device: *In Vitro* and *In Vivo* Fluorescence Studies[1]

Sarah J. Erickson, Jiajia Ge, Andrea Sanchez and Anuradha Godavarty

Department of Biomedical Engineering, Florida International University, Miami, FL 33174, USA

Abstract

Near-infrared (NIR) optical imaging is a noninvasive and nonionizing modality that is emerging as a diagnostic tool for breast cancer. The handheld optical devices developed to date using the NIR technology are predominantly developed for spectroscopic applications. A novel handheld probe–based optical imaging device has been recently developed toward area imaging and tomography applications. The three-dimensional (3D) tomographic imaging capabilities of the device have been demonstrated from previous fluorescence studies on tissue phantoms. In the current work, fluorescence imaging studies are performed on tissue phantoms, *in vitro*, and *in vivo* tissue models to demonstrate the fast two-dimensional (2D) surface imaging capabilities of this flexible handheld-based optical imaging device, toward clinical breast imaging studies. Preliminary experiments were performed using target(s) of varying volume (0.23 and 0.45 cm^3) and depth (1-2 cm), using indocyanine green as the fluorescence contrast agent in liquid phantom, *in vitro*, and *in vivo* tissue models. The feasibility of fast 2D surface imaging (~5 seconds) over large surface areas of 36 cm^2 was demonstrated from various tissue models. The surface images could differentiate the target(s) from the background, allowing a rough estimate of the target's location before extensive 3D tomographic analysis (future studies).

Translational Oncology (2010) 3, 16–22

Introduction

Handheld-based optical imaging devices have been developed for breast imaging to accelerate the clinical translation of the technology toward cancer diagnosis. Several of these handheld devices have been tested *in vivo* on human subjects [1 2 3 4 5, selected publications]. However, they are unable to contour to the curvature of human breast tissue because all these devices used flat-probe faces. The predominant applications to date have been either toward spectroscopic measurement of tissue optical properties or two-dimensional (2D) localization studies of abnormal tissue within the breast. Recently, a handheld optical imaging device has been developed in our Optical Imaging Laboratory [6] toward imaging large tissue surfaces using a flexible probe face that contours to different tissue curvatures. The device is intended to augment current clinical imaging modalities for breast cancer detection and diagnosis. The three-dimensional (3D) tomographic ability of the device has been demonstrated on large tissue phantoms using a fluorescence-enhanced–based imaging technique [7]. Herein, preliminary studies are performed on tissue phantoms, *in vitro*, and *in vivo* tissue models to demonstrate the fast 2D surface imaging capabilities of this flexible handheld-based optical imaging device toward clinical breast imaging studies.

Materials and Methods

Instrumentation

The instrumentation for the handheld optical imaging device consists of a 785-nm, 500-mW laser diode source and an intensified charge-coupled device (ICCD) camera detector (with 550-850 nm bandwidth at the intensifier end) as shown in Figure 1. The source light is launched onto and collected from the tissue surface using a handheld-based probe head (4 × 9-cm^2 imaging area). The handheld probe consists of 6 points of illumination and 165 points of collection (as shown in Figure 2) of optical signals through optical fibers, which connect the probe head to the source and detector. The total

Address all correspondence to: Anuradha Godavarty, Department of Biomedical Engineering, Florida International University, Optical Imaging Laboratory, 10555 W Flagler St, EC 2675, Miami, FL 33174. E-mail: godavart@fiu.edu

[1]The authors thank the Florida Department of Health (08BB-06) and Department of Defense (BC083282) for their funding support.
Received 6 June 2009; Revised 8 September 2009; Accepted 15 September 2009

DOI 10.1593/tlo.09157

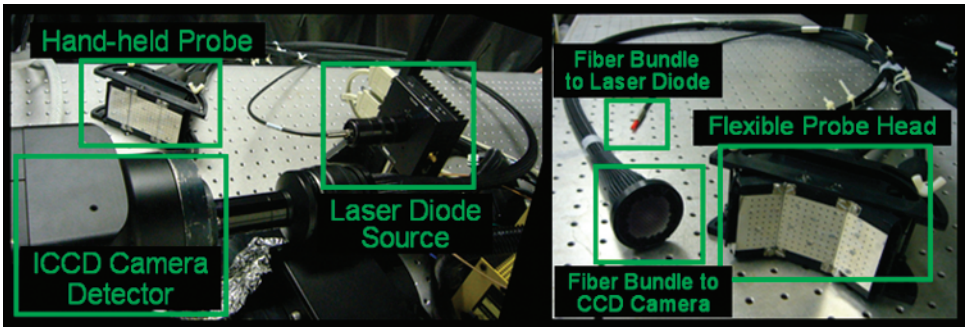

Figure 1. Handheld probe–based optical imaging system showing the handheld probe is fiber-optically coupled to the laser source and ICCD camera (left). The probe face is flexible to contour to different tissue curvatures (right).

laser power incident on the phantom or tissue is <10 mW. The device has a flexible probe head design such that it contours to different tissue curvatures during imaging. Simultaneous illumination and detection from multiple point locations is carried out to reduce the overall imaging time. Additional details of the instrumentation are provided elsewhere [7]. The instrumentation is developed such that it can acquire both continuous wave (CW)–based and frequency-domain–based optical measurements as required. To facilitate 2D imaging in real time, the device was operated in the CW mode for the current study in tissue phantoms, *in vitro*, and *in vivo*.

Data Acquisition and Analysis

Two-dimensional surface imaging was performed, using the handheld device operated in the CW mode, on tissue phantoms, *in vitro*, and *in vivo* tissue models. In all cases, fluorescence-enhanced imaging was performed using an external fluorescing agent indocyanine green (ICG) for improved contrast. Spherical acrylic targets (of different sizes) filled with 1 μM ICG were used to mimic a tumor. The target was placed at different depths from the imaging surface and different target-to-background (T:B) contrast ratios (1:0 and 100:1) were used for different experimental cases. The probe was placed in contact with the phantom or tissue surface as shown in Figure 3, and CW images of the fluorescent intensity were acquired in close to real time (~2 seconds' delay). The raw fluorescence intensity images at the ICCD camera end were acquired in 1 second (0.2-second exposure time × 5 repetitions). These images were postprocessed (~1 second) using in-house developed Matlab codes to acquire the final 2D surface contour plots of fluorescence intensity distribution of the imaged surface. The entire data acquisition and postprocessing were automated such that close to real-time (~2 seconds' delay) imaging is possible. The 2D surface contour plots of fluorescence intensity signal may or may not differentiate the target from the tissue phantom background, based on the target and background optical properties.

During fluorescence optical imaging, the output signal at the tissue surface is a mixture of fluorescence signal and the attenuated incident near-infrared (NIR) (i.e., excitation) signal. This fluorescence signal is filtered from the strong excitation signal (three to four orders of magnitude higher) using appropriate optical (band-pass) filters and imaged by the detector. However, the filters are not capable of 100% rejection of the excitation light, causing an excitation leakage and contamination of the fluorescent signal. Hence, a second level of postprocessing is carried out to subtract a background nonfluorescing image from the final fluorescence image plots for each experimental case to account for the excitation leakage. Initially, optical measurements were acquired before placing the fluorescent target in the phantom, in an attempt to represent the excitation leakage (or background noise). These (background noise) measurements were subtracted from the fluorescence optical measurements obtained from experimental cases that included fluorescent targets to effectively eliminate the signal from the excitation source light. In the clinical setting involving actual diseased tissues (unlike the simulated fluorescent targets in the current study), this could be accomplished by acquiring image(s) of the tissue before and after the contrast agent (e.g., ICG) injection. The nonfluorescent image(s) acquired before ICG injection will in turn be subtracted from the fluorescent images acquired after ICG injection to account for the background noise.

The subtracted 2D fluorescence images are generated rapidly (<5 seconds), making the entire process a fast 2D surface imaging technique. The acquisition of these subtracted fluorescence 2D surface contour plots has greater significance in 2D target localizations as well as in 3D tomographic imaging studies.

Experimental Cases

Tissue phantom studies. Studies were performed using slab tissue phantoms composed of 10 × 10 × 10-cm^3 acrylic cubes filled with 650 ml of 1% Liposyn solution (Liposyn II, 20%; Henry Schein, Melville, NJ) to mimic the optical properties of a typical breast tissue. The fluorescent target was placed at different depths (1.5-2.5 cm) from

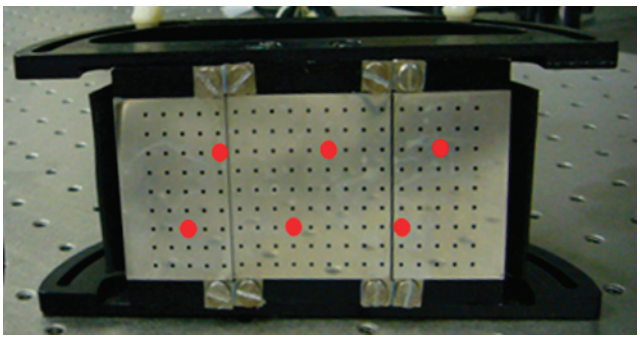

Figure 2. Picture of the handheld probe face showing the source-detector configuration. The large red dots represent the six source fiber locations, and all other small holes are the 165 detector fiber locations.

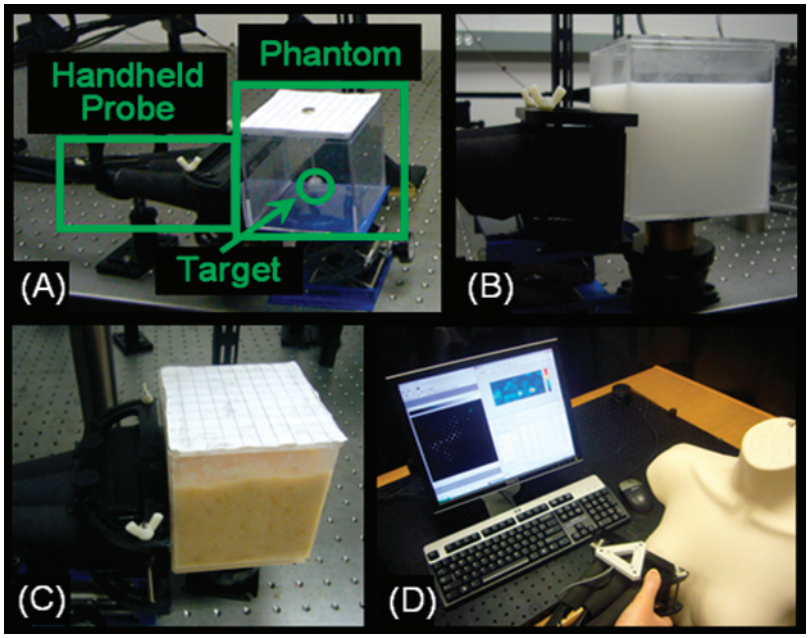

Figure 3. Experimental setup for tissue phantom, *in vitro*, and *in vivo* studies: (A) empty phantom showing target inclusion and placement of probe, (B) tissue slab phantom with 1% Liposyn solution for uniform scattering in the background, (C) *in vitro* slab phantom with heterogeneous scattering in the background, and (D) setup for *in vivo* studies using mannequin (for demonstration only) to represent human subject.

the imaging surface and real-time as well as fast (subtracted) images of fluorescence intensity were acquired. The different experimental cases are summarized in Table 1.

In vitro phantom studies. Before *in vivo* studies with human subjects, experiments were performed using *in vitro* phantoms, which were composed of minced chicken breast combined with 1% Liposyn solution, to introduce a nonuniform scattering background. The *in vitro* mixture of minced chicken breast (480 ml) and 1% Liposyn (260 ml) was placed inside a 10 × 10 × 10-cm^3 acrylic cube. Real-time as well as fast (subtracted) images of fluorescence intensity were acquired under different experimental conditions using either a 0.23-cm^3 or 0.45-cm^3 fluorescent target located at various depths between 1 and 2 cm (Table 1).

In vivo studies. *In vivo* studies were performed on healthy human subjects to demonstrate the feasibility of using the handheld device to collect images of a fluorescent target with a background of real human breast tissue. All human subject studies were approved by the Florida International University Institutional Review Board. Healthy female volunteers aged 21 and older were recruited for the studies. A fluorescent target was used to simulate a tumor (as described in Data Acquisition and Analysis) and was placed underneath the flap of the breast tissue (i.e. between breast tissue and chest wall, underneath the tissue). In the first study, a 0.23-cm^3 sphere with 1 μM ICG was placed under the right breast in the 4-o'clock position. The flat-probe face was placed against the breast tissue with gentle compression, and a real-time fluorescent intensity image was acquired (around the target region). The depth of the target within the tissue was approximately 2.5 cm as measured with a vernier caliper.

A second study was performed using a single target with the probe in the maximum curved position (i.e., 45° curvature of the two side plates of the three-plate–based probe face). The images collected with the probe in the curved position possibly include transilluminated measurements in addition to reflectance-based measurements. This study was performed to demonstrate the feasibility of using the probe

Table 1. Summary of Experimental Cases for Slab Tissue Phantom, *In Vitro*, and *In Vivo* Studies.

Subject Studied	Experiment No.	Number of Targets	Target Depth (cm)	Target Volume (cm^3)	T:B Contrast Ratio
Slab tissue phantom (uniform scattering in background)	1	1	1.5	0.45	1:0
	2	1	2.0	0.45	1:0
	3	1	2.5	0.45	1:0
In vitro phantom (nonuniform scattering in background)	4	1	1.0	0.45	1:0
	5	1	1.5	0.45	1:0
	6	1	2.0	0.45	1:0
	7	1	1.0	0.23	1:0
	8	1	1.5	0.23	1:0
	9	1	2.0	0.23	1:0
In vitro with healthy human subject	10	1	2.5	0.23	1:0
	11	1	2.5	0.45	1:0
	12	2	2.5	0.23 and 0.45	1:0

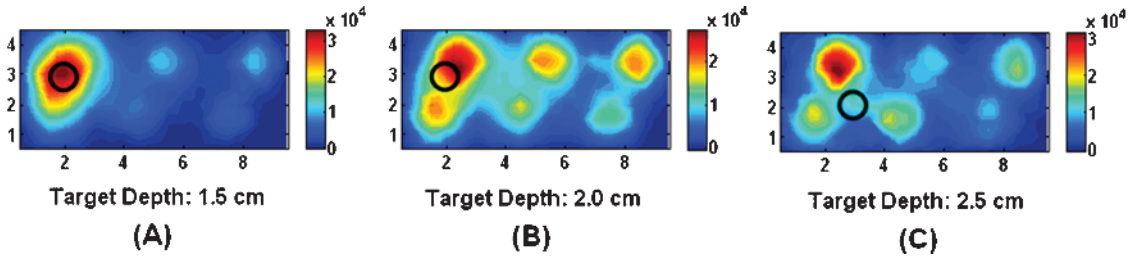

Figure 4. Near real-time images of fluorescence intensity obtained as 2D surface contour plots acquired from slab phantoms (with uniform background scattering). The fluorescent target was placed at different locations and depths: (A) target location (x,y,z) = (2.0, 2.7, 1.5), and (B) target location (x,y,z) = (2.0, 2.7, 2.0), and (C) target location (x,y,z) = (3.0, 2.2, 2.5). The black hollow circle in each subplot is the true target location.

in its curved position, such that it can contour along the tissue and also provide fluorescent images that can aid in target detection. Herein, a 0.45-cm^3 fluorescent target containing 1 μM ICG was placed under the right breast in the 8-o'clock position. A real-time as well as fast (subtracted) image of fluorescence intensity was acquired by applying gentle compression along the tissue curvature.

A third study was performed to demonstrate the feasibility of imaging multiple targets within real human breast tissue. Two targets were placed under the fold of the left breast tissue, with a 0.23-cm^3 target at the 6-o'clock position, and a 0.45-cm^3 target was placed at the 8-o'clock position of the same breast. A real-time as well as fast (subtracted) image of fluorescence intensity was acquired by applying gentle compression on the left breast tissue.

All these preliminary *in vivo* studies used micromolar concentrations of ICG in the tumor-mimicking target(s), similar to the current tissue phantom, *in vitro* phantom studies, and also that used by other researchers [7–9]. The actual *in vivo* studies on breast cancer subjects cannot estimate the concentration of ICG (after injection) at the tumor site, and the researchers typically report the injected quantities of the contrast agent [8,10].

Results

Tissue Phantom Studies

Real-time images using the slab phantom with uniform scattering in the background are shown in Figure 4 as 2D surface contour plots of the fluorescence intensity data with a target placed at different depths (1.5-2.5 cm) from the imaging surface. The nonuniform intensity distribution in Figure 4 is possibly due to the residual excitation leakage around the six source fibers (after the implementation of the subtraction technique). In addition, the input laser source signal is not evenly distributed among the six source fibers, possibly causing a variation or nonuniformity in the output fluorescence intensity distribution.

The images show the feasibility of performing (close to) real-time 2D imaging using the handheld device in tissue phantoms. The actual target location in the images is indicated in the figures by the black open circle in the *x-y* plane for different target depths in the "*z*" direction. The fast 2D image estimates the 2D target location (instantly) in the *x-y* plane. This information can then be further used toward 3D tomography (in the future) to determine the tumor volume, location, and depth [9].

From these plots, it is obvious that the real-time images are capable of differentiating the target from the background when the 0.45-cm^3 target was 1.5 cm deep. At greater tissue depths, the target was not distinctly differentiable because of the strong excitation leakage from the background. On applying the subtraction technique (as described in Data Acquisition and Analysis), the target is clearly differentiable from the background in all the experimental cases (Figure 5). These subtracted images also have potential to obtain 3D target localization through tomographic imaging, as long as the probe's location on the tissue surface is coregistered with respect to the surface fluorescence images.

In Vitro *Phantom Studies*

The results for the *in vitro* phantom experiments are shown in Figures 6 (real-time images) and 7 (fast subtracted images) for different target depths (1-2 cm) under a T:B contrast ratio of 1:0. The true

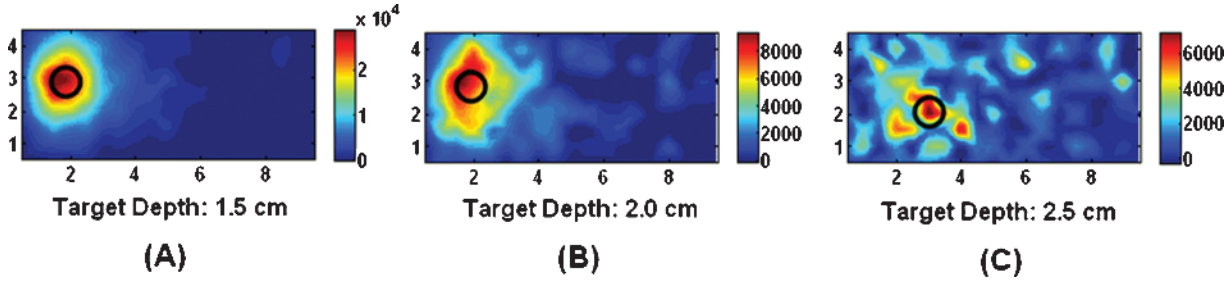

Figure 5. Fast subtracted images of fluorescence intensity obtained as 2D surface contour plots acquired from slab phantoms (with uniform background scattering). The 0.45-cm^3 fluorescent target was placed at different locations and depths: (A) target location (x,y,z) = (2.0, 2.7, 1.5), and (B) target location (x,y,z) = (2.0, 2.7, 2.0), and (C) target location (x,y,z) = (3.0, 2.2, 2.5). The black hollow circle in each subplot is the true target location.

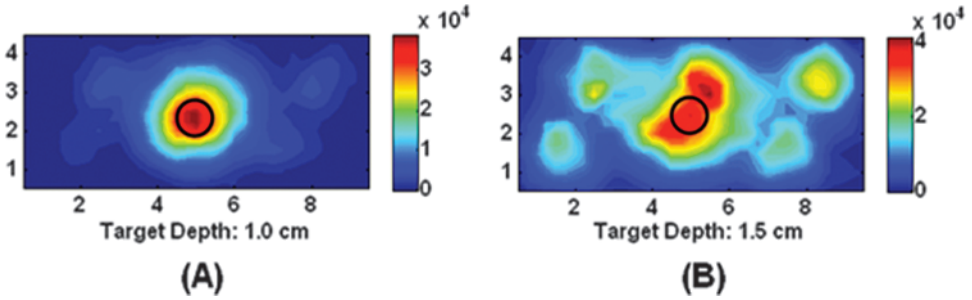

Figure 6. Near real-time images of fluorescence intensity obtained as 2D surface contour plots acquired from *in vitro* slab phantoms (with nonuniform background scattering). The 0.45-cm^3 fluorescent target was located at a depth of (A) 1.0 cm and (B) 1.5 cm from the imaging surface. The black hollow circle in each subplot is the true target location.

target location in the images is given as *x*,*y*,*z* coordinates where "*x*" is the lateral position, "*y*" is the height, and "*z*" is the depth that vary among the images. Owing to heterogeneous scattering of the background phantom, only the subtracted images were capable of clearly differentiating the target from the background for targets deeper than 1.0 cm. These studies show the ability of the handheld device to perform fast 2D surface imaging and target localization within a nonuniform scattering tissue-mimicking background.

In Vivo *Studies*

Figure 8 shows the fast 2D subtracted images of fluorescence intensity obtained *in vivo* (from a healthy human subject using a simulated target) with the probe in the flat position (Figure 8*A*) and in the curved position (Figure 8*B*). These subtracted image results demonstrate the feasibility of fast 2D surface imaging and 2D target localization in a clinical environment. The real-time (nonsubtracted) images of fluorescence intensity were unable to differentiate the target from the heterogeneous background, and hence, only the fast 2D subtracted images are shown in Figure 8.

The 2D subtracted images of fluorescent intensity from multiple simulated targets in a human subject are shown in Figure 9. The 0.23-cm^3 target is detected in the center of the image and the 0.45-cm^3 target is detected toward the left side in the image, which are very close to the true locations of these targets. This study demonstrates the potential to image and localize multiple fluorescent targets (of different sizes) within human breast tissue.

Discussion

The fluorescence imaging studies described here demonstrate for the first time the acquisition of fast 2D surface images (in <5 seconds) of a fluorescent target in uniform tissue phantoms, *in vitro*, and *in vivo* using a handheld-based optical imaging device. The subtracted images have a potential to clearly differentiate target(s) from the background (under various experimental conditions), demonstrating the potential to translate the technology toward on-site breast imaging in a clinical environment. Additional experiments were performed with the target located at greater depths in the tissue phantoms, but the target was not detected at a depth of 2.5 cm. At 2.5 cm deep, the

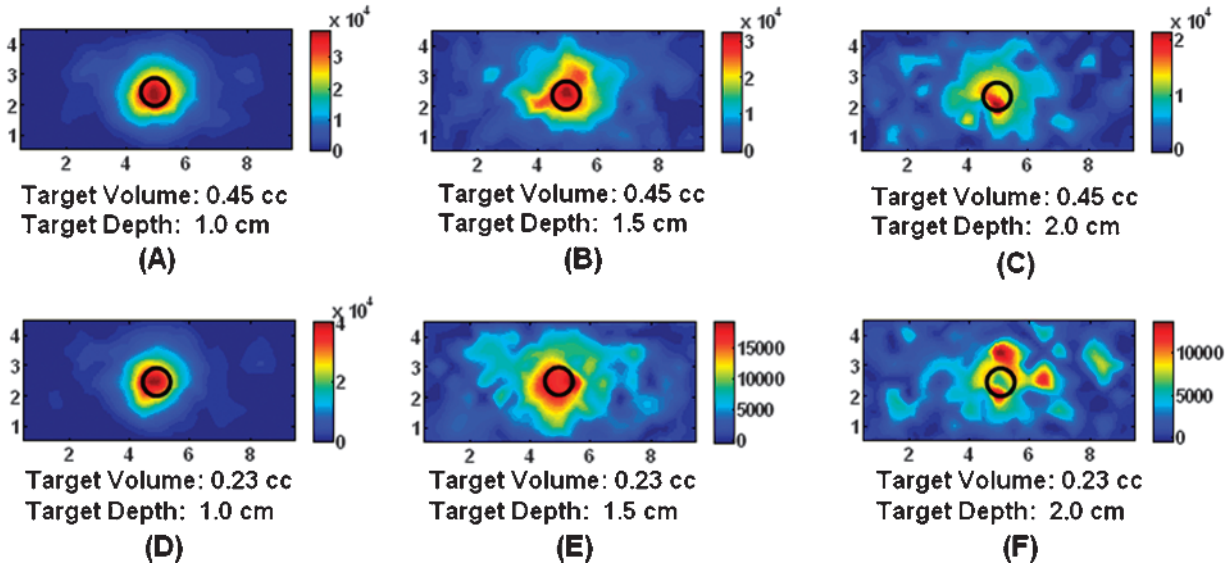

Figure 7. Fast subtracted images of fluorescence intensity obtained as 2D surface contour plots acquired from *in vitro* slab phantoms (with nonuniform background scattering). Images were collected for different target sizes and depths. Images (A) to (C) contain a target size of 0.45 cm^3 at depths of 1.0, 1.5, and 2.0 cm, respectively. Images (D) to (F) contain a target size of 0.23 cm^3 at depths of 1.0, 1.5, and 2.0 cm, respectively. The black hollow circle in each subplot is the true target location.

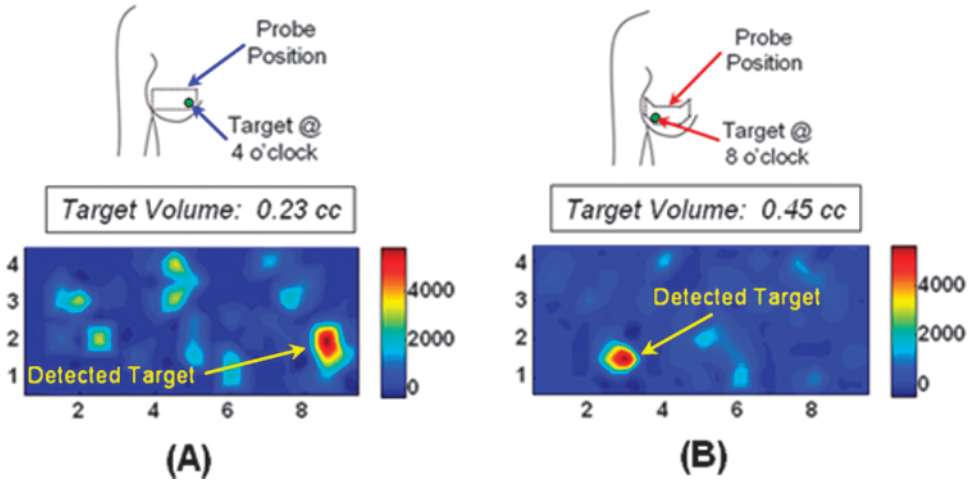

Figure 8. Fast subtracted images of fluorescence intensity obtained as 2D surface contour plots, acquired *in vivo* from a human subject using a spherical fluorescent target, for two experimental cases: (A) the probe was in the flat position and a 0.23-cm^3 target was placed at the 4-o'clock position; and (B) the probe was in the curved position and a 0.45-cm^3 target was placed at the 8-o'clock position. The images acquired using the probe in the curved position are illustrated as projected as a flat 2D image to be consistent with the images presented in case (A) (i.e., using the probe in flat position).

detected signal from the target is close to the noise floor and hence not differentiable from the background. A multilocation scanning approach is currently developed in our laboratory for differentiating deeply located or small-volume targets from homogenous or heterogeneous background [11]. In short, this approach will incorporate the use of coregistered images obtained at multiple locations on the tissue surface, such that the targets can be differentiated from artifacts as well as the background [11]. When comparing Figures 4 and 5, it can be seen that the images from the *in vitro* phantom contain more noise than those from the uniform tissue phantom. This can possibly be attributed to the heterogeneous distribution of scattering properties or shifting of the chicken breast as the target is removed (which can cause a change in the signal distribution when the background image is collected). Experiments were also performed using the *in vitro* phantoms with a T:B contrast ratio of 100:1. However, the noise from the background signal dominated the image, and a target was not detected even after subtracting the excitation background signal. On applying our multilocation scanning approach, the targets were differentiable under imperfect uptake conditions (i.e., T:B = 100:1) [11]. In addition to fast 2D imaging, the handheld device described here has demonstrated 3D tomography of fluorescent targets with tissue phantoms using frequency-domain–based measurements to estimate the 3D location and volume of the target within the tissue [9]. Our ongoing efforts will involve the implementation of fast and automated coregistration facilities to enable precise 2D target localization (instantaneously) as well as 3D tomography studies (*in vitro* as well as *in vivo*).

Conclusions

A handheld-based optical imaging device has been developed in our Optical Imaging Laboratory toward *in vivo* clinical studies on breast

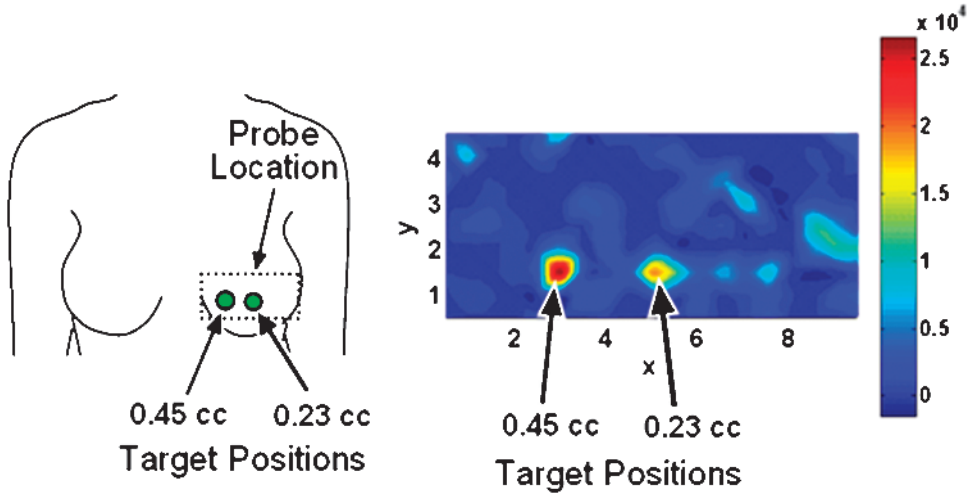

Figure 9. Fast subtracted image of fluorescence intensity obtained as 2D surface contour plot acquired *in vivo* from a human subject using two spherical fluorescent targets (0.23 and 0.45 cm^3).

tissues. The device has been tested extensively in the past on homogeneous slab phantoms (with sample results shown here). The device has been tested for CW-based fluorescence optical imaging *in vitro* as well as *in vivo*. The fluorescence studies demonstrate the ability of the handheld device to perform fast 2D imaging and also detect a fluorescent target within a heterogeneous tissue-mimicking background as well as real human breast tissue (on using subtracted images). Future work will involve fast coregistered imaging of human breast tissue to enable 3D tomography in human subjects using this novel handheld-based optical device.

References

[1] Cerussi AE, Berger AJ, Bevilacqua F, Shah N, Jakubowski D, Butler J, Holcombe RF, and Tromberg BJ (2001). Sources of absorption and scattering contrast for near-infrared optical mammography. *Acad Radiol* **8**, 211–218.

[2] Shah N, Cerussi AE, Jakubowski D, Hsiang D, Butler J, and Tromberg BJ (2004). Spatial variations in optical and physiological properties of healthy breast tissue. *J Biomed Opt* **9** (3), 534–540.

[3] Cerussi A, Shah N, Hsiang D, Durkin A, Butler J, and Tromberg BJ (2006). *In vivo* absorption, scattering, and physiologic properties of 58 malignant breast tumors determined by broadband diffuse optical spectroscopy. *J Biomed Opt* **11** (4), 044005.

[4] Chance B, Nioka S, Zhang J, Conant EF, Hwang E, Briest S, Orel SG, Schnall MD, and Czerniecki BJ (2005). Breast cancer detection based on incremental biochemical and physiological properties of breast cancers: a six-year, two-site study. *Acad Radiol* **12** (8), 925–933.

[5] Zhu Q, Cronin EB, Currier AA, Vine HS, Huang M, Chen NG, and Xu C (2005). Benign *versus* malignant breast masses: optical differentiation with US-guided optical imaging reconstruction. *Radiology* **237**, 57–66.

[6] Jayachandran B, Ge J, Regalado S, and Godavarty A (2007). Design and development of a hand-held optical probe toward fluorescence diagnostic imaging. *J Biomed Opt* **12** (5), 054014.

[7] Godavarty A, Eppstein MJ, Zhang C, Theru S, Thompson AB, Gurfinkel M, and Sevick-Muraca EM (2003). Fluorescence-enhanced optical imaging in large tissue volumes using a gain modulated ICCD camera. *Phys Med Biol* **48** (12), 1701–1720.

[8] Corlu A, Choe R, Durduran T, Rosen MA, Schweiger M, Arridge SR, Schnall MD, and Yodh AG (2007). Three-dimensional *in vivo* fluorescence diffuse optical tomography of breast cancer in humans. *Opt Express* **15** (11), 6696–6716.

[9] Ge J, Zhu B, Regalado S, and Godavarty A (2008). Three-dimensional fluorescence-enhanced optical tomography using a hand-held probe based imaging system. *Med Phys* **35** (7), 3354–3363.

[10] Sevick-Muraca EM, Sharma R, Rasmussen JC, Marshall MV, Wendt JA, Pham HQ, Bonefas E, Houston J, Sampath L, Adams KE, et al. (2008). Imaging of lymph flow in breast cancer patients after microdose administration of a near-infrared fluorophore: feasibility study. *Radiology* **246** (3), 734–741.

[11] Regalado S, Zhu B, Ge J, Erickson SJ, and Godavarty A (in press). Automated coregistered imaging using a hand-held probe-based optical imager. *Rev Sci Inst*.